Biomass Valorization Hot Paper

How to cite: *Angew. Chem. Int. Ed.* **2020**, *59*, 20508 – 20514
International Edition: doi.org/10.1002/anie.202003236
German Edition: doi.org/10.1002/ange.202003236

Dynamics of Ligand Binding to a Rigid Glycosidase**

*Fredj Ben Bdira, Christopher A. Waudby, Alexander N. Volkov, Sybrin P. Schröder, Eiso AB, Jeroen D. C. Codée, Hermen S. Overkleeft, Johannes M. F. G. Aerts, Hugo van Ingen, and Marcellus Ubbink**

Abstract: *The single-domain GH11 glycosidase from Bacillus circulans (BCX) is involved in the degradation of hemicellulose, which is one of the most abundant renewable biomaterials in nature. We demonstrate that BCX in solution undergoes minimal structural changes during turnover. NMR spectroscopy results show that the rigid protein matrix provides a frame for fast substrate binding in multiple conformations, accompanied by slow conversion, which is attributed to an enzyme-induced substrate distortion. A model is proposed in which the rigid enzyme takes advantage of substrate flexibility to induce a conformation that facilitates the acyl formation step of the hydrolysis reaction.*

Introduction

Glycoside hydrolases (GH) play essential roles in multiple biological processes, including the degradation of polysaccharides as sources of energy, the modulation of the cellular glycoconjugates to mediate cellular communications, host-pathogen interactions, signal transduction, inflammation and intracellular trafficking.[1] These highly efficient catalysts can enhance the rate of glycosidic bond hydrolysis by a factor of more than 10^{17},[2] which makes them valuable tools for biotechnological applications, such as in biofuel production, paper pulp bleaching and food industry.[3] Probing the role of structure and dynamics in substrate conversion can provide new insights into the workings of these enzymes and pave the way for efficient biotechnological and therapeutic utilization.

Among GH families are the ubiquitous retaining β-glycosidases, which employ "Koshland" double displacement mechanism for catalysis.[4] These glycosidases often have highly ordered structures. It has been suggested that rigidity is required for substrate binding and distortion to facilitate hydrolysis.[5] To establish the enzyme rigidity and characterize the interactions with the substrate in solution, we studied several forms of the enzyme xylanase from *Bacillus circulans* (BCX), mimicking the intermediates of the enzyme catalyzed reaction. In the crystalline state, structures of BCX in the resting state and various complexes are essentially identical, suggesting that no conformational changes occur during the catalytic steps [root mean square deviations (RMSD) of the Cα atoms ≈ 0.1 Å and ≈ 0.4 Å for all heavy atoms] (Supporting Information, Figure S1A). BCX features the conserved β-jelly roll fold that derives its rigidity from an extensive intramolecular hydrogen bond network involving 146 out of its 185 backbone amides, resulting in restricted dynamics on the pico-nanosecond time scale for the resting state.[5b] The shape of BCX is often compared to a right-hand fist, which includes "hand palm", "fingers" and "thumb" regions (Figure 1). The active site of the protein includes six subsites to bind units of the β 1–4 xylose polymer xylan, three (−) subsites (glycon binding site) and three (+) subsites (aglycon binding site), according to the nomenclature of Davies et al.[6] (Figure 1C). The glycosidic bond hydrolysis takes place between the $-1/+1$ subsites with a substrate binding in at least the $-2/-1$ and $+1$ subsites, in accordance with an *endo*-

[*] Dr. F. Ben Bdira, Dr. H. van Ingen, Prof. Dr. M. Ubbink
Department of Macromolecular Biochemistry
Leiden Institute of Chemistry
Einsteinweg 55, 2333 CC Leiden (The Netherlands)
E-mail: m.ubbink@chem.leidenuniv.nl
Dr. C. A. Waudby
Institute of Structural and Molecular Biology
University College London and Birkbeck College
London WC1E 6BT (UK)
Dr. A. N. Volkov
VIB-VUB Center for Structural Biology
Pleinlaan 2, 1050 Brussels (Belgium)
Dr. A. N. Volkov
Jean Jeener NMR Centre, VUB
Pleinlaan 2, 1050 Brussels (Belgium)
Dr. S. P. Schröder, Prof. Dr. J. D. C. Codée, Prof. Dr. H. S. Overkleeft
Department of Bio-organic Synthesis, Leiden Institute of Chemistry
Einsteinweg 55, 2333 CC Leiden (The Netherlands)
Dr. E. AB
ZoBio BV, BioPartner 2 building
J.H. Oortweg 19, 2333 CH Leiden (The Netherlands)
Prof. Dr. J. M. F. G. Aerts
Department of Medical Biochemistry, Leiden Institute of Chemistry
Einsteinweg 55, 2333 CC Leiden (The Netherlands)
Dr. H. van Ingen
Present address: NMR Spectroscopy Research Group
Bijvoet Center for Biomolecular Research, Utrecht University
Padualaan 8, 3584 CH Utrecht (The Netherlands)

[**] A previous version of this manuscript has been deposited on a preprint server (https://www.biorxiv.org/content/10.1101/815415v1).

Supporting information, including Materials and Methods, Figures S1–S8, Tables S1–S4, References (1–12), and the ORCID identification number(s) for the author(s) of this article can be found under:
https://doi.org/10.1002/anie.202003236.

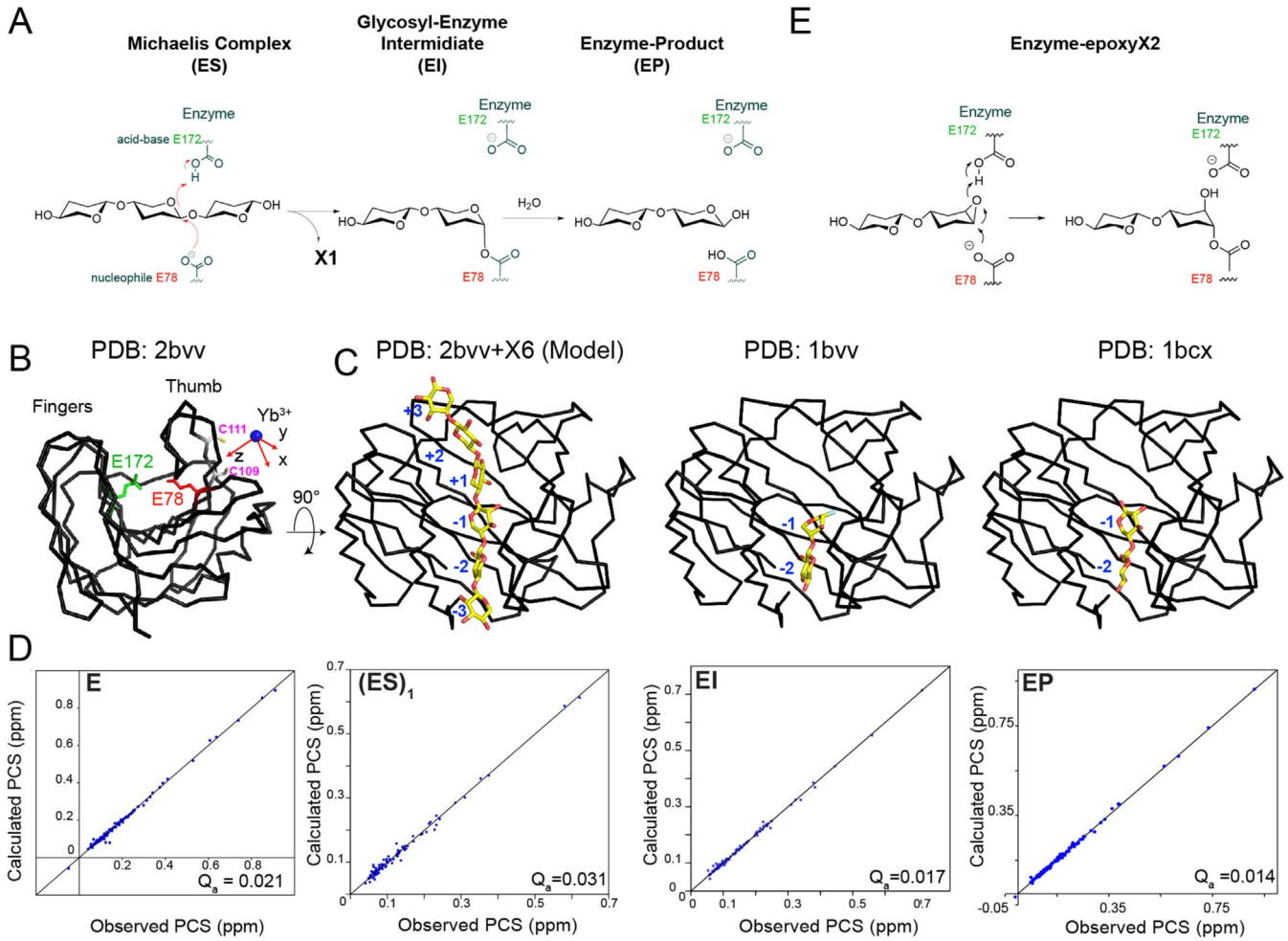

Figure 1. BCX structural analysis of the crystalline and solution states for several steps along the enzymatic pathway. A) "Koshland" double displacement retaining mechanism. B) Crystal structure of resting state BCX (state E) shown as black Cα trace (PDB:2bvv).[10] The nucleophile (E78, red) and acid-base (E172, green) catalytic dyad are shown in sticks. The location of the lanthanoid (blue sphere) in the CLaNP-5 tag and the tensor $\Delta\chi$ (red arrows) defined by the anisotropic component of the magnetic susceptibility are shown. Cysteines used for CLaNP tagging are in sticks. C) Structures of BCX, from left to right, model of the ES complex based on the structure of XynII bound to X6 (PDB: 4hk8)[11] in which the substrate binding subsites are numbered (−3/+3); EI complex (PDB: 1bvv)[10] and EP complex (PDB:1bcx).[12] The RMSD values for the Cα atoms relative to the resting state are ≈0.1 Å for all structures. D) Correlation plots of the experimental PCS of the E, $(ES)_1$, EI and EP states fitted to the crystal structure of resting state BCX (PDB: 2bvv), indicating that this structure is a good model for these catalytic states in solution. Fitting to the crystal structures of the intermediate states does not improve the fit. E) BCX-EI covalent complex formation by epoxyX2. The inactivation mechanism involves the attack of the ligand epoxide active center by the enzyme nucleophile, resulting in ring opening and the formation of a covalent bond between the enzyme nucleophile and the inhibitor, which emulates the EI state of the natural substrate hydrolysis reaction. The process is facilitated by protonation of the inactivator reactive center by the general acid/base residue.

catalytic mechanism. BCX is a retaining β-glycosidase using a nucleophile and an acid/base catalytic dyad, proceeding through the non-covalent (Michaelis) complex (ES), covalent intermediate (EI) and product complex (EP) states (Figure 1 A).[7] Crystal structures representing these states are shown in Figure 1 C. We probed structures that mimic these states, using paramagnetic NMR spectroscopy. In parallel, we determined the dynamic behavior of BCX on the millisecond timescale with relaxation dispersion NMR spectroscopy (RD-NMR). Though some minor dynamics is observed in loop regions, the core of the enzyme, including the active site, is rigid and does not exhibit structural changes in the successive complexes. The substrate binds rapidly in many orientations and in parallel, a longer-lived enzyme-substrate complex is detected, which is attributed to a state in which the bound substrate is distorted.

Results and Discussion

The structure of BCX in solution does not change during the enzymatic cycle. Pseudocontact shifts (PCS) are a useful NMR tool to probe backbone conformation changes of proteins in solution, because PCS are highly conformation dependent.[8] The PCS of amide nuclei of the different states were obtained with a BCX variant that has two engineered cysteine residues (T109C/T111C) linked to a lanthanoid tag (CLaNP-5),[9] containing either a paramagnetic Yb^{3+} ion or

a Lu^{3+} ion as a diamagnetic control (Figure 1B; Figures S1B,C). In the resting state, BCX shows an excellent agreement between solution and crystalline state structures, as revealed by the fit of the PCS to the protein crystal structure (PDB: 2bvv)[10] (Figure 1D). The same crystal structure was also able to fit the PCS obtained for the three other states (ES, EI and EP, see below), indicating that the structural changes in the backbone of the enzyme are minimal throughout the enzymatic cycle in solution, in line with the results for the crystalline states. Though the anisotropic nature and strong distance dependence of the PCS prevents the definition of a uniform detection limit for structural changes, based on a comparison of two structures with a different conformation of the thumb region, it seems reasonable to state that changes in amide positions of ≥ 2 Å would likely have been detected (Figures S1D,E).

Substrate and product interactions with BCX. Upon titration of a catalytically inactive variant of BCX-E78Q with the substrate xylohexaose (X6), mimicking the Michaelis complex, a complicated chemical shift perturbation (CSP) pattern was observed. BCX is known to bind substrate in the active site, as well as in a secondary binding site (SBS) on the surface of the protein.[13] The backbone and side chain amides of the SBS residues exhibit large CSP in the fast exchange regime (Figure 2A; Figure S2A). CSP in and around the cleft of the active site are small but widespread (Figure 2A; Figure S2A). These CSP are also in the fast exchange regime and several of the amides display progressive line broadening during the titration. The remarkable difference in the sizes of the CSP between the two binding sites suggests a difference in the substrate binding modes. The SBS is a relatively flat region, exposed to the surface, which makes it accessible to

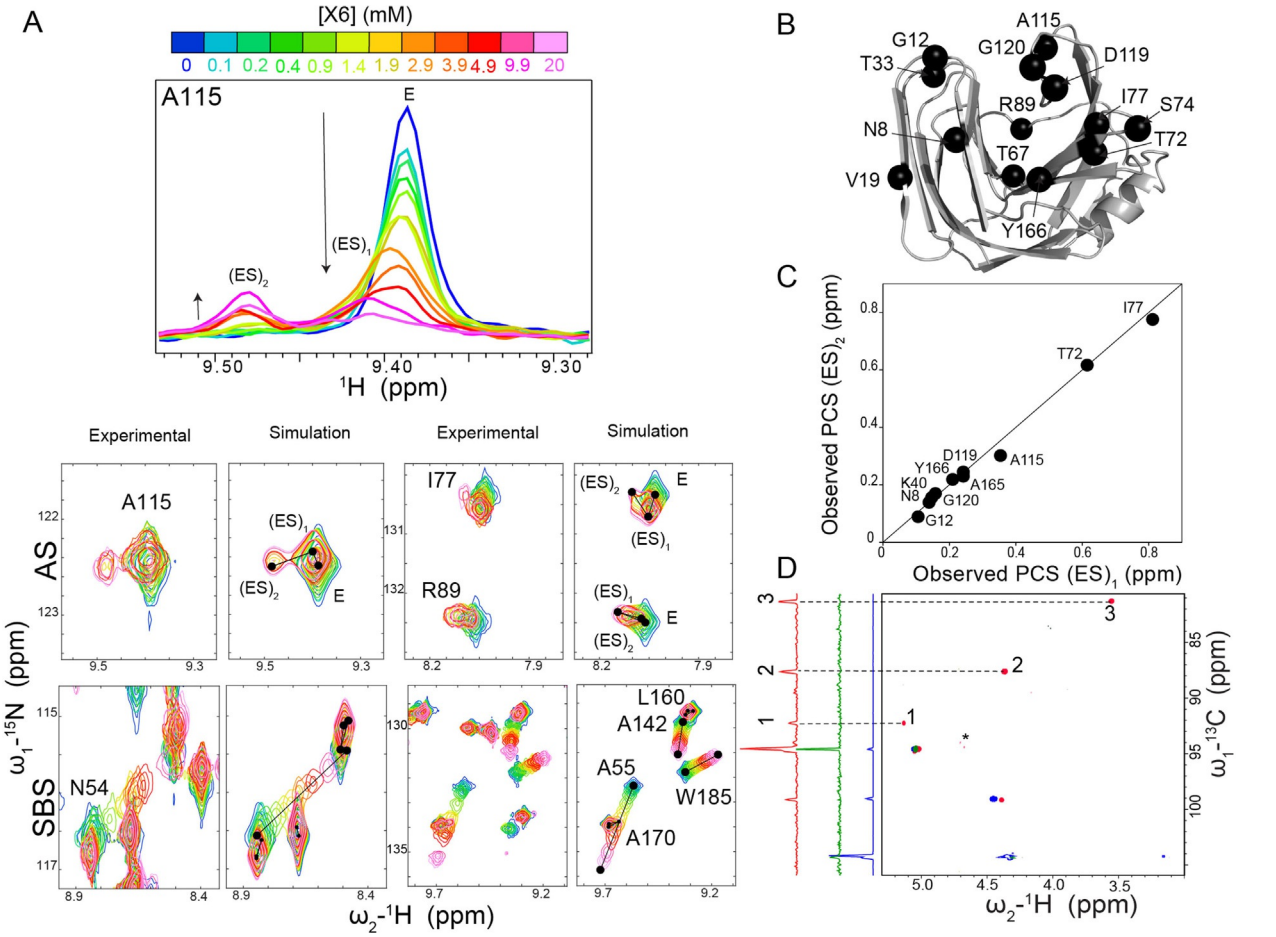

Figure 2. BCX-E78Q Michaelis complex formation. A) In the upper panel BCX-E78Q ^{1}H-^{15}N HSQC ^{1}H slices are displayed for residue A115, showing that its amide resonance position and intensity changes with the appearance of its new peak in the $(ES)_2$ state upon titration with X6. Note that at the highest concentrations of X6 a general line broadening occurred due to an increase in solution viscosity (Figure S3C). In the lower panel, CSP of BCX-E78Q backbone amides in the active site (AS) and SBS are shown next to simulated spectra using the binding model described in M&M and implemented in TITAN software[20] (see M&M and Figure S3). B) Amide groups with additional peaks representing the $(ES)_2$ state are shown in black spheres on BCX crystal structure. C) Correlations between the experimental PCS of the $(ES)_1$ and $(ES)_2$ states. D) Overlay between the free X6 ^{1}H-^{13}C HSQC spectrum (1500 μM in blue); in the presence of 480 μM (in green) and 1500 μM of BCX-E78Q (in red). The 1D projections of the ^{1}H-^{13}C HSQC spectra of each condition are shown on the left side of the spectrum using the same color code. The emerging X6 peaks are numbered and connected to the 1D projections with dashed lines. The asterisk marks the residual water signal. On the basis of the binding parameters obtained from the global fit (Table S2), it is estimated that the concentrations $(ES)_1$ and $(ES)_2$ are 74 and 44 μM, and 192 and 115 μM for the samples with 480 μM and 1500 μM BCX-E78Q, respectively (neglecting an allosteric effect).

the substrate to bind in a well-defined orientation causing large CSP.[13] In contrast, the active site is formed by a deep cleft filled with water molecules, with six subsites. It is expected that the substrate can bind in multiple "registers", that is, shifted along the subsequent subsites and perhaps also in reverse orientation. The averaged effect of these different binding modes will be small CSP over a wide area, due to changes in the hydrogen bond network between the amides and the water molecules.[14]

Interestingly, for residues in the substrate-binding cleft of the active site a new set of resonances becomes observable at [X6] = 3.9 mM (Figure 2A). This observation indicates that a second form of the enzyme-substrate complex, $(ES)_2$, is present, which is in slow exchange with a first form, $(ES)_1$. Although for many amides such new peaks appear, only those close to existing resonances could be assigned reliably using PCS, and these resonances are from nuclei in the binding cleft (Figure 2B). At higher ligand concentrations ([X6] = 10, 20 mM) a decrease of peak intensity for $(ES)_1$ resonances and increase for $(ES)_2$ resonances is observed (Figure 2A). A global fit of the lineshapes of the SBS and active site amides resonances (Figure 2A; Figure S3) shows that X6 binding and release from the SBS is quite fast ($k_{ex} = 7.8 \times 10^4\ s^{-1}$ at [X6] = 20 mM, $k_{ex} = k_{on}[X6] + k_{off}$). Also, the binding of X6 in the active site is in the fast regime on the NMR timescale, albeit eight-fold slower than for the SBS ($k_{ex} = 0.9 \times 10^4\ s^{-1}$ at [X6] = 20 mM). The fitting model included X6 binding at two sites, the SBS and active site, as well as a slow conversion of $(ES)_1$ into $(ES)_2$ (M&M; Supporting Information, Table S2). While the model fits most aspects of the titration well, it did not account for the increase of the $(ES)_2/(ES)_1$ ratio at the high concentrations of X6. This increase indicates that the $(ES)_2$ state, being the state with an X6 molecule in the active site in conformation 2, becomes more populated when a second X6 molecule occupies the SBS, suggesting an allosteric effect of X6 binding in the remote SBS on the active site. Inclusion of such effect in the modelling led to overfitting and, thus it could not be modeled reliably. Interestingly, it has been reported before that the longer substrates xylododecaose (X12), as well as soluble and insoluble xylan, can bind to the active site and SBS simultaneously with a single substrate molecule, reducing the K_m of the enzyme.[13] Thus, information transfer between the SBS and active site appears to be possible. The $(ES)_1$ and $(ES)_2$ states exchange at a rate of 71 s^{-1} ($k_{ex} = k_{forward} + k_{backward}$). This exchange rate is in the range of the turn-over rate of BCX using the artificial substrate PNP-X2 (20 s^{-1}, 23 °C) for which the glycosylation step has been shown to be rate limiting.[15] Assuming that the $(ES)_2$ state is relevant for enzyme turnover; our findings suggest that the conversion of $(ES)_1$ into $(ES)_2$ could be rate limiting. A similar slow process was reported for a different type of glycosidase, chitosanase, when titrated with chitosan hexaose.[16] In that study, the slow exchange was attributed to a conformational change of the protein induced by ligand binding. However, for BCX-E78Q the similarity of the PCS of resonances in $(ES)_1$ and $(ES)_2$ indicates that the conversion from $(ES)_1$ to $(ES)_2$ does not lead to a major structural rearrangement of the enzyme (Figure 2C).

This observation poses the question what the slow transition step in BCX-E78Q Michaelis complex represents. We wondered if a conformational change in the bound substrate could be the cause of the two ES states. To test this hypothesis, we observed the effects of BCX-E78Q binding on X6 by using ^1H-^{13}C HSQC NMR experiments at natural abundance to detect nuclei of the sugar rings. Many of the ^{13}C resonances lie in a region of the spectrum (75–105 ppm) in which the protein shows no resonances. Upon addition of BCX-E78Q, the resonances of many X6 resonances shift and broaden beyond detection, even at a BCX-E78Q:X6 ratio of 0.2:1 (Figure S2D), in line with the model formulated above, in which X6 molecules bind and dissociate rapidly in different modes and thus exhibit different chemical shifts, both to the SBS and the active site. Then, the ratio of BCX-E78Q and X6 was increased to 1:1 (1.5 mM each). Interestingly, several new peaks were detected in the region of the sugar resonances, indicating the presence of another form of X6 that is not affected by the fast-exchange binding events (Figure 2D). Thus, this observation is analogous to the observation of the additional peaks observed for the BCX-E78Q amides, the $(ES)_2$ state. The ^{13}C chemical shifts of the new peaks differ considerably (> 10 ppm) from those of the free sugar, indicating that the new form must experience significant conformational change or its electronic environment is strongly affected by the enzyme. A crystal structure of X6 bound to another GH11 xylanase, XynII-E177Q (PDB: 4hk8) shows that the oligosaccharide chain is in a well-defined, yet strained conformation.[11] This structure could represent the equivalent of the BCX-E78Q $(ES)_2$ structure, in solution. Chemical shift predictions of this distorted form did not differ significantly from those for the relaxed conformation of the sugar ring, suggesting that either the distorted form observed by NMR differs or that the protein environment has a strong effect on the ^{13}C chemical shifts of the sugar. The authors suggest that this state could be primed for catalysis. A computational study supported the observation that the substrate is distorted, but it suggested that the conformation of the sugar at the −1 subsite of the E177Q mutant differs from the one adopted in the wild type enzyme.[17] Thus, using the BCX-E78Q mutant it is not possible to state with certainty whether the experimentally observed distorted forms are catalytically on-route or off-route structures.

To mimic the next step in the catalytic cycle, the covalent intermediate state, a covalent inhibitor (epoxyX2) was used that resembles xylobiose (X2)[18] (Figure 1E). Despite the absence of structural changes in the enzyme (see above), adduct formation leads to many CSP (Figure S2B), which are attributed to changes in the hydrogen bond network in and around the active site due to binding of the adduct and displacement of water molecules. These observations are reminiscent with the noted dramatic change in the pK_a value of the acid/base residue upon formation of the 2-fluoro-β-xylobioside glycosyl enzyme complex.[19]

The last step of the reaction is product release from the glycon pocket after hydrolysis. A NMR titration of BCX with X2, representing the product, shows that ligand binding is again in the fast exchange regime, with $k_{ex} = 4.3 \times 10^4\ s^{-1}$ at [X2] = 130 mM (Figure S2E). No additional peaks in the slow

exchange regime were observed at high ligand concentration, contrary to the titration with X6. X2 also does not interact with the SBS to a detectable level. Based on the CSP pattern, the ligand appears to occupy only the −1/−2 subsites (Figure S2C), indicative of a difference in the binding sites affinities between the glycon and aglycon sites toward the product.

Substrate and product binding enhance exchange effects. RD-NMR experiments were performed to detect lowly populated states that are in dynamic equilibrium with the ground states. RD-NMR on the resting state of BCX show that millisecond chemical exchange is limited to residues located within the fingers and the thumb regions, with few residues affected in the active site (Figures S4A and S5A). A two-site exchange model fit of the dispersion data yields a $k_{ex} = 2.4(\pm 0.1) \times 10^3\ s^{-1}$ (20 °C) and a population of the excited state p_B of 0.8 % (Table S3). It is noted that a two-site exchange model is the simplest case and it may represent an oversimplification.[21] The analysis is used here to estimate the order of magnitude of the k_{ex} and p_B. For the EI complex, the chemical exchange effects mostly resemble those for the resting state BCX, both qualitatively and quantitatively ($k_{ex} = 2.05(\pm 0.08) \times 10^3\ s^{-1}$, p_B of 0.6 %; Figures S4C and S5B, Table S3). Large exchange broadening effects (R_{ex} up to 50 s^{-1}) were observed for both the Michaelis complex $(ES)_1$ and the product complex (EP) for amino acid residues that form the binding cleft (Figure 3). A two-site exchange fit yielded $k_{ex} = 741(\pm 9)\ s^{-1}$, $p_B = 9.2(\pm 0.2)$ % for $(ES)_1$ and $k_{ex} = 1.53(\pm 0.02) \times 10^3\ s^{-1}$, $p_B = 4.00(\pm 0.04)$ % for EP (Figures S4B,D, Table S3). In the EP complex, large R_{ex} values were found in particular for amide nitrogen atoms of the thumb and fingers at the −1/−2 subsites, which also experience CSP upon ligand titration (Figure S2C) and were reported to have a large perturbing effect on the pK_a values of the acid/base and nucleophile.[19]

Origin of chemical exchange effects in the non-covalent complexes. Crystal structures of BCX in various states, as well as the PCS analysis, indicate that BCX shows negligible conformational changes during turnover, raising the question what conformations the excited states observed in the RD-NMR experiments represent and whether they are relevant for enzyme function. For other enzymes, the evidence that excited states represent conformations of the next state in the enzymatic cycle has been obtained by showing a correlation between the ^{15}N chemical shifts of excited states, derived from the $\Delta\omega$ values of RD NMR experiments, with those of the successive ground states.[22] Such a correlation could not be found for the data reported here (Figure S6), in line with a similar analysis on a BCX related protein, XlnB2.[23] The combination of a lack of enzyme conformational changes and the strong enhancement of the chemical exchange for the states in which the enzyme interacts non-covalently with substrate or product molecules ($(ES)_1$ and EP states), suggests the presence of multiple binding modes of the substrate in the active site. As mentioned above, it can be expected that both X6 and X2 can bind in different "registers" and positions of the six binding subsites, with different affinities. Each binding mode would change the hydrogen bond network of amides

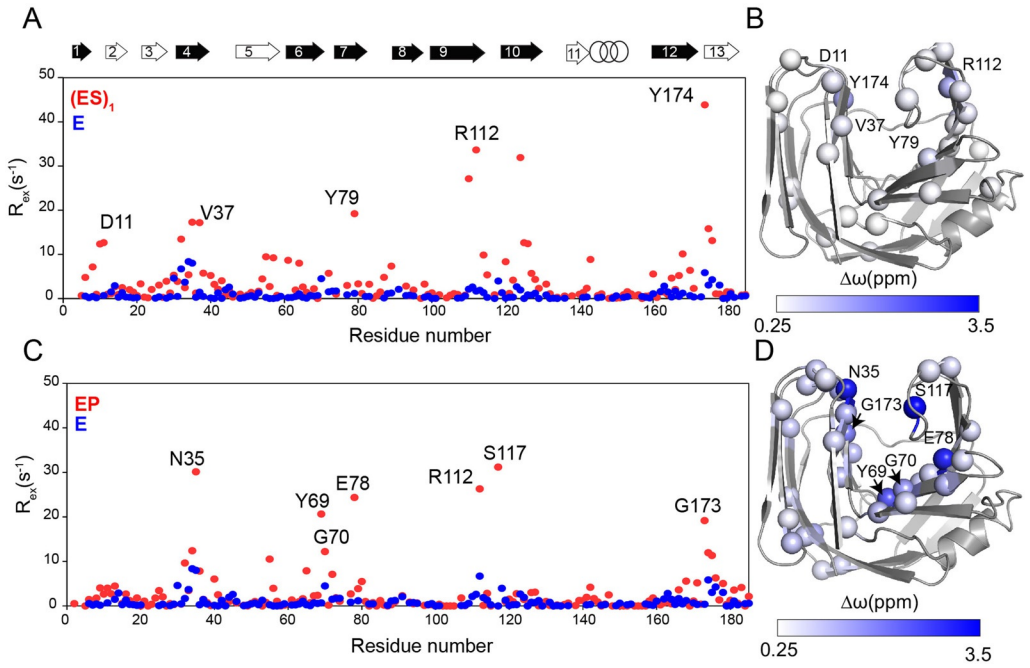

Figure 3. Non-covalent interactions enhance BCX millisecond time scale dynamics in the $(ES)_1$ and EP states. A,C) Overlay of the R_{ex} values of $(ES)_1$ (A) or EP (C) (red dots) and E states (blue dots) plotted versus the residue number. Several residues that show a prominent difference in R_{ex} are labeled. The secondary structure elements of BCX are represented by black arrows for β-strands of sheet A and in white ones for sheet B and the α-helix in rings. The "thumb" loop connects β-strands 9 and 10. B,D) Amide nitrogen atoms used in the RD global fit for $(ES)_1$ (B) and EP (D) are shown in spheres on the BCX crystal structure (PDB ID: 2bvv) colored by their $\Delta\omega$ between the ground and excited states, using a white/blue gradient. The $\Delta\omega$ were derived from a global two-state fit to the dispersion curves.

and waters in the active site in a different way and, thus, cause different CSP. The presence of multiple binding modes in $(ES)_1$ can explain the observed chemical exchange in the active site. The NMR titration results for $(ES)_1$ formation indicated rapid association and dissociation ($k_{ex} \approx 10^4\ s^{-1}$), which would be too fast to yield RD effects. However, the exchange between bound states via the free state can still be sufficiently slow to cause chemical exchange broadening, as shown in the M&M and Table S4 for a simple case with two binding modes, $(ES)_1$ and $(ES)_1$*. The fact that in the resting enzyme the affected amides are in loop regions outside the active site in conjunction to the very low population of its excited states suggests that the millisecond enzyme dynamics may not be relevant for substrate binding or product release. Note that this does not exclude much higher-frequency, vibrational dynamics (femtosecond) playing a role in the actual chemical reaction, as suggested by Schramm et al.[24]

All the NMR results can be integrated in a model describing the successive states of the enzymatic cycle, Figure 4. The titration results indicate rapid association of BCX and X6 into the non-covalent complex $(ES)_1$, in the enzyme binding cleft. The substrate can bind in multiple modes, resulting in different $(ES)_1$ complexes, causing the observed RD effects for the amides in the active site. One or more of $(ES)_1$ complexes can proceed to form $(ES)_2$, with a high activation barrier, because the conversion is slow. This conversion is attributed to the substrate distortion in the active site without inducing conformational rearrangement in the protein, an 'induced fit of the substrate'. The rate of conversion between $(ES)_1$ and $(ES)_2$ is in the range of the turnover rate of the enzyme, so $(ES)_2$ it could represent an activated form of the ES complex that can proceed rapidly to form the EI complex. After hydrolysis, the product complex (EP) is in fast exchange with the free enzyme and product, as shown by the NMR titration, and, analogous to the $(ES)_1$ complex, the product can bind in various modes, resulting in multiple EP complexes, as evidenced by the RD effects for this complex.

Conclusion

In conclusion, xylanase from *B. circulans* is an enzyme with few conformational changes during the different steps of the enzymatic cycle. X6 can bind in multiple modes with different affinities and high dissociation rates. A slow transition occurs in the substrate-bound state and we propose that this represents a distortion of the substrate in the active site, representing an on-route and perhaps rate-limiting event of the enzymatic reaction. We note, however, that further evidence for such role is needed, because we worked with a catalytically inactive mutant. On the basis of the data we cannot exclude that the distorted form is off-route, implying that either (one of the) $(ES)_1$ complexes or another distorted form that only occurs with the wild type enzyme would be the reactive complex. The enzyme appears to provide a rigid frame that stabilizes specific substrate conformations to enable the reaction to proceed. The observed dynamics in the Michaelis complex are attributed to multiple substrate binding modes within the active site. Most of the GH11 family members are secreted enzymes,[25] which function under harsh extracellular conditions, thus, a rigid matrix that is able to take advantage of the inherent conformational landscape of the substrate, may offer evolutionary advantages.

Acknowledgements

We thank Professor Lewis E. Kay for providing us with the TROSY-CPMG pulse program. We thank Thomas Hansen for performing DFT computations. This work was supported by the NWO research school NRSCB, grant number 022.004.027 (H.S.O). C.A.W was supported by Wellcome Trust (WT), grant number 206409/Z/17/Z.

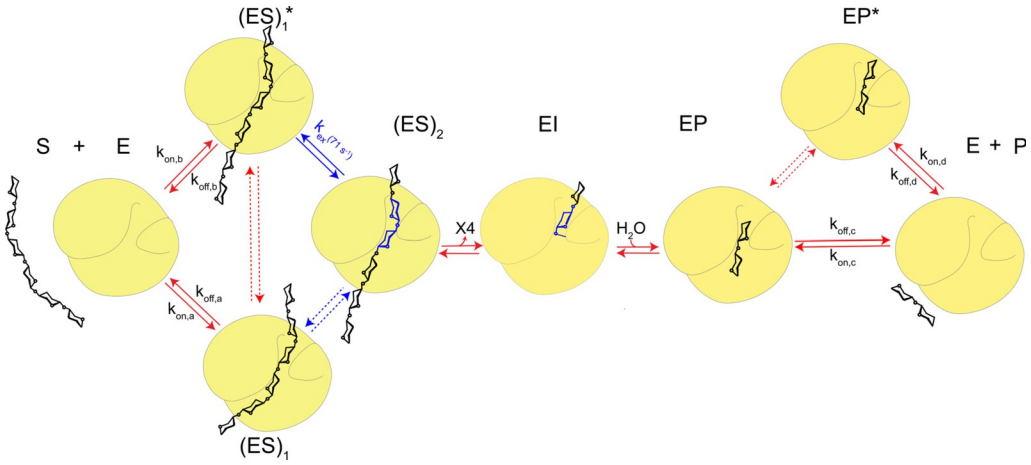

Figure 4. Proposed model for BCX enzymatic cycle. Blue sugar units indicate X6 distortion. Possible values for the microscopic rates $k_{on,\,i}$ and $k_{off,\,i}$ that yield the experimental dissociation rates, exchange rates, minor state populations and dissociation constants are given in Table S4. Dashed arrows indicate equilibria that could be present but for which no experimental evidence was obtained. In the model, the substrate X6 and X2 can bind in multiple ways, forming a major state and one or more minor state(s), indicated with an asterisk.

Conflict of interest

The authors declare no conflict of interest.

Keywords: dynamics · glycosidases · ligand binding · NMR spectroscopy · rigid fold

[1] K. Kato, A. Ishiwa, *Trop. Med. Health* **2015**, *43*, 41 – 52.
[2] R. Wolfenden, X. Lu, G. Young, *J. Am. Chem. Soc.* **1998**, *120*, 6814 – 6815.
[3] a) S. Garg, *Curr. Metabolomics* **2016**, *4*, 23 – 37; b) L. Viikari, A. Kantelinen, J. Sundquist, M. Linko, *FEMS Microbiol. Rev.* **1994**, *13*, 335 – 350; c) Â. S. M. Miguel, T. S. Martins-Meyer, E. Figueiredo, B. W. P. Lobo, G. M. Dellamora-Ortiz, *Food Ind.* **2013**, 278 – 321.
[4] D. Koshland, Jr., *Biol. Rev.* **1953**, *28*, 416 – 436.
[5] a) D. K. Poon, M. L. Ludwiczek, M. Schubert, E. M. Kwan, S. G. Withers, L. P. McIntosh, *Biochemistry* **2007**, *46*, 1759 – 1770; b) G. P. Connelly, S. G. Withers, L. P. Mcintosh, *Protein Sci.* **2000**, *9*, 512 – 524; c) F. B. Bdira, M. Artola, H. S. Overkleeft, M. Ubbink, J. M. Aerts, *J. Lipid Res.* **2018**, *59*, 2262 – 2276; d) V. Rojas-Cervellera, A. Ardèvol, M. Boero, A. Planas, C. Rovira, *Chem. Eur. J.* **2013**, *19*, 14018 – 14023; e) A. White, D. Tull, K. Johns, S. G. Withers, D. R. Rose, *Nat. Struct. Mol. Biol.* **1996**, *3*, 149 – 154.
[6] G. J. Davies, K. S. Wilson, B. Henrissat, *Biochem. J.* **1997**, *321*, 557.
[7] S. L. Lawson, W. W. Wakarchuk, S. G. Withers, *Biochemistry* **1997**, *36*, 2257 – 2265.
[8] C. Nitsche, G. Otting, *Prog. Nucl. Magn. Reson. Spectrosc.* **2017**, *98 – 99*, 20 – 49.
[9] a) P. H. Keizers, A. Saragliadis, Y. Hiruma, M. Overhand, M. Ubbink, *J. Am. Chem. Soc.* **2008**, *130*, 14802 – 14812; b) P. H. Keizers, J. F. Desreux, M. Overhand, M. Ubbink, *J. Am. Chem. Soc.* **2007**, *129*, 9292 – 9293.
[10] G. Sidhu, S. G. Withers, N. T. Nguyen, L. P. McIntosh, L. Ziser, G. D. Brayer, *Biochemistry* **1999**, *38*, 5346 – 5354.
[11] Q. Wan, Q. Zhang, S. Hamilton-Brehm, K. Weiss, M. Mustyakimov, L. Coates, P. Langan, D. Graham, A. Kovalevsky, *Acta Crystallogr. Sect. D* **2014**, *70*, 11 – 23.
[12] W. W. Wakarchuk, R. L. Campbell, W. L. Sung, J. Davoodi, M. Yaguchi, *Protein Sci.* **1994**, *3*, 467 – 475.
[13] M. L. Ludwiczek, M. Heller, T. Kantner, L. P. McIntosh, *J. Mol. Biol.* **2007**, *373*, 337 – 354.
[14] M. P. Williamson, *Prog. Nucl. Magn. Reson. Spectrosc.* **2013**, *73*, 1 – 16.
[15] D. L. Zechel, L. Konermann, S. G. Withers, D. Douglas, *Biochemistry* **1998**, *37*, 7664 – 7669.
[16] S. Shinya, M. G. Ghinet, R. Brzezinski, K. Furuita, C. Kojima, S. Shah, E. L. Kovrigin, T. Fukamizo, *J. Biomol. NMR* **2017**, *67*, 309 – 319.
[17] J. Iglesias-Fernández, L. Raich, A. Ardèvol, C. Rovira, *Chem. Sci.* **2015**, *6*, 1167 – 1177.
[18] S. P. Schröder, R. Petracca, H. Minnee, M. Artola, J. M. F. G. Aerts, J. D. C. Codée, G. A. van der Marel, H. S. Overkleeft, *Eur. J. Org. Chem.* **2016**, 4787 – 4794.
[19] M. D. Joshi, G. Sidhu, J. E. Nielsen, G. D. Brayer, S. G. Withers, L. P. McIntosh, *Biochemistry* **2001**, *40*, 10115 – 10139.
[20] C. A. Waudby, A. Ramos, L. D. Cabrita, J. Christodoulou, *Sci. Rep.* **2016**, *6*, 24826.
[21] D. M. Korzhnev, K. Kloiber, L. E. Kay, *J. Am. Chem. Soc.* **2004**, *126*, 7320 – 7329.
[22] a) D. D. Boehr, D. McElheny, H. J. Dyson, P. E. Wright, *Science* **2006**, *313*, 1638 – 1642; b) E. Z. Eisenmesser, D. A. Bosco, M. Akke, D. Kern, *Science* **2002**, *295*, 1520 – 1523.
[23] D. Gagné, C. Narayanan, N. Nguyen-Thi, L. D. Roux, D. N. Bernard, J. S. Brunzelle, J.-F. Couture, P. K. Agarwal, N. Doucet, *Biochemistry* **2016**, *55*, 4184 – 4196.
[24] V. L. Schramm, S. D. Schwartz, *Biochemistry* **2018**, *57*, 3299 – 3308.
[25] P. Rapp, F. Wagner, *Appl. Environ. Microbiol.* **1986**, *51*, 746 – 752.

Manuscript received: March 3, 2020
Revised manuscript received: May 29, 2020
Accepted manuscript online: June 13, 2020
Version of record online: September 3, 2020

